Investigation of Mercury Wet Deposition Physicochemistry in the Ohio River Valley through Automated Sequential Sampling

Emily M. White[1*], *Gerald J. Keeler*[2], *James A. Barres*[2],

Matthew S. Landis[1]

[1] U.S. EPA Office of Research and Development, Research Triangle Park, North Carolina 27711

[2]University of Michigan Air Quality Laboratory, Ann Arbor, Michigan 48109

*Corresponding author phone: (919)541-0361

ABSTRACT

Intra-storm variability and soluble fractionation was explored for summer-time rain events in Steubenville, Ohio, with the intent of evaluating the physical processes controlling mercury (Hg) in wet deposition in this industrialized region. Comprehensive precipitation sample collection was conducted from July through September 2006 using several different methods to evaluate both soluble and insoluble fractions as well as scavenging and washout properties of Hg and a suite of trace elements. Real-time filtration of event total precipitation revealed that 61 ± 17% of Hg in wet deposition was in a soluble form. Hg, along with the other measured trace elements show the following order of decreasing solubility: S > Na > Se > Ca > Mg > Hg > As > Mn > V > Cr> Fe > La ≈ Ce ranging from 95% (S) to 4% (Ce). In order to examine removal mechanisms during the course of a precipitating event, discrete sequential sub-event precipitation samples were collected. Results indicated that Hg had lower "scavenging coefficients" (the rate of Hg concentration decrease throughout the events) than the majority of elements analyzed, indicating that either (i) Hg is incorporated into rain via gas phase inclusion or particulate nucleation within cloud, (ii) or Hg is available in the boundary layer for scavenging, even in the

latter stages of precipitation. The Hg scavenging coefficient was particularly low compared to S, a co-pollutant of Hg, with the highest scavenging coefficient. When compared to an upwind, regionally representative site, the scavenging coefficient of Hg for the locally influenced precipitation was significantly lower. This observation suggests that a continuous feed of soluble Hg is the reason for the low scavenging coefficient. Overall, this investigation of Hg wet deposition in Steubenville indicates that the physicochemical properties of Hg emissions result in elevated deposition rates near point sources.

Keywords: atmospheric mercury, local source impact, mercury scavenging coefficient

1 INTRODUCTION

1.1 Background

The mercury (Hg) wet deposition flux to Eastern Ohio has been shown to be enhanced over other US regions due to local and regional anthropogenic point sources (Keeler et al, 2006; White et al, 2009). Hg wet deposition has been correlated to methylmercury concentrations in fish, a critical step in the bioaccumulation process of this hazardous neurotoxin (Hammerschmidt and Fitzgerald, 2006). With international policy decisions regarding mitigation of Hg emissions currently under negotiation, the best possible understanding of biogeochemical cycling of Hg is essential.

The means by which a pollutant enters precipitation is exceptionally dynamic, involves several possible processes, and is determined by numerous parameters. For example, with pollutant species in both gas and particle forms, there is conversion from one form to another (homogeneous and heterogeneous), and the particles on which the pollutant is bound can act directly as cloud condensation nuclei via nucleation scavenging. Soluble gases can diffuse into cloud droplets within cloud or below clouds in rain drops. Primarily coarse mode particles can also be scavenged by falling precipitation below cloud. The specific process that dominates at any one time depends on several factors: pollutant concentration, speciation, species solubility, conversion rates, moisture content, reactive gas concentrations, size distribution of particles, UV availability, temperature, and air parcel height. It should also be noted that warm versus cold cloud microphysics play a major role in pollutant entrainment: in warm cloud processes small, ionic heterogeneous nucleation dominates while ice particle nucleation prefers larger lattice-type nuclei, such as soil and biogenic particles (Houze, 1993). Snow and mixed precipitation are less effective scavengers of Hg (Landis et al, 2002). Here, we focus on summer-time warm processes, as the vast majority of Hg wet deposition in the Steubenville area is in the form of rain (White et al, 2009).

Spatial modeling of Hg deposition fluxes is a multidimensional problem due to substantial gaps in our understanding of atmospheric chemistry and deposition processes of Hg, and the scarcity of speciated Hg measurements from many types of emission point sources. Gaseous Hg is present in the atmosphere in two major inorganic forms: elemental Hg (Hg^0), and divalent

(Hg^{2+}) often referred to as reactive gaseous mercury (RGM) or reactive oxidized mercury (ROM). Hg adhered to particles is referred to as particulate Hg (Hg(p)). While the global pool is >99% Hg^0, emissions from point sources may range from 25 – 90% Hg^{2+} (Lindberg, 2007). Hg^0 is very low in solubility and therefore removed slowly after oxidation and subsequent incorporation into wet deposition. Hg^{2+} is removed rapidly because of its relatively high solubility and affinity to surface reactions. Consequently, transformations between the oxidation states (Hg^0 oxidizes to Hg^{2+} in the presence of OH, O_3, and halides and is hypothesized that Hg^{2+} may reduce to Hg^0 in point source plumes and clouds (Lindberg, 2007)) and emissions speciation will determine deposition rates.

It has been noted that wet deposition monitoring networks that are designed to be regionally representative do not adequately address near field deposition enhancement and the resulting spatial variability of Hg deposition in the vicinity of urban and industrial centers (Dvonch et al, 1998, Van Metre, 2012, Sherman et al, 2012). Recent work has shown a distinctly steep Hg wet deposition gradient in the vicinity of Coal-Fired Utility Boilers (CFUBs), with near field samples exhibiting up to 72% enhancement in Hg concentrations (White et al, 2009) over those sampled at locally and regionally representative sites. This near field Hg deposition enhancement is typically not reflected in contemporary deterministic model output, and it is apparent that a better fundamental understanding of atmospheric Hg chemistry and the physicochemical drivers affecting the incorporation of Hg into precipitation is needed to adequately parameterize models.

One way to experimentally determine removal mechanisms is to evaluate pollutant concentrations over the course of a single precipitation event. Sequential sampling of particles, major ions and total trace metals during a wet deposition event may aid in determining the removal mechanisms of analytes (Gatz and Dingle, 1971; Coscio et al, 1982; Lim et al, 1990; Krupa, 2002). Previous studies have linked the relative cumulative deposition rates of the various constituents to removal processes: certain constituents were removed by below-cloud processes as indicated by the rapid removal rate; in-cloud particle accumulation mechanisms fell into mid-range deposition rates, followed by very low cumulative deposition rates, indicative of gas phase within-cloud scavenging of gases (Lim et al, 1990; Krupa, 2002). There is no published literature specifically pertaining to sequential sampling of Hg or the removal mechanisms therein. The solubility fractionation of heavy metals in precipitation has been

discussed and deemed important both for flux determinations as well as bioavailability properties (Lou, 2001; Morselli et al, 2003; Graney et al, 2004); it is hypothesized that by a first approximation, the fraction of an element dissolved in deposited precipitation is the most available for interaction with living organisms (Morselli et al, 2003; Sandroni and Migon, 2002). Experimentally, it has been shown that Hg becomes bioavailable for microbial methylation when in the dissolved state (Benoit et al, 2001). Inorganic Hg deposition is methylated through the uptake by anaerobic organisms in aquatic ecosystems, and understanding the parameters driving methylation rates including the fraction of soluble Hg deposition that is readily available for this process are critically important.

1.2 Previous Study Results

A general descriptive analysis of daily event sampled Hg wet deposition for Steubenville, OH as well as the Lake Michigan and Lake Champlain areas results can be found in the literature (Landis et al., 2002; Keeler et al, 2006; White et al, 2009; Gratz and Keeler, 2011; White et al., 2012). Four key findings have direct relevance to this work:

(i) The variabilty in event total Hg concentration is related to precipitation depth (amount of precipitation), a general decreasing trend in Hg concentration with sample size is evident, and this relationship differs by precipitation type (rain, snow or mixed). The strength of this relationship is influenced by degree of local source influence; the washout coefficient (linear regression slope of the natural log of Hg concentration versus depth) is lowest for samples collected at sites in close proximity to known Hg sources. At four regionally representative sites in the midwest US and at Lake Champlain VT, the coefficient is consistently reported at -0.23 to -0.24 (Landis et al, 2002; Gratz et al, 2005). In the Chicago/Gary urban/industrial area, the coefficient droped to -0.16, indicating that local source strength may be an important factor driving the variation in Hg concentration amoung event samples (Landis et al., 2002), as large samples were not necessarily diluted.

(ii) At the Steubenville study site, summertime (July and August) precipitation accounts for approximately 30% of the yearly Hg wet deposition flux (White et al, 2009).

(iii) Receptor modeling found greater than 70% of total Hg in wet deposition at the Steubenville study site could be attributed to coal combustion (Keeler et al, 2006; White et al., 2012). As part of the analysis, it was determined that wet deposited S and Se were the primary tracers of coal combustion, with 76 and 71% attributed to that factor, respectively (Keeler et al, 2006; White et al., 2012).

(iv) 42% of the Hg in precipitation samples collected in the immediate vicinity of CFUBs was attributed to the adjacent sources (White et al., 2009). This spatial gradient is not well captured in contemporary deterministic models, indicating that there are significant gaps in our understanding of Hg physicochemistry, how it relates to the emissions-to-deposition cycle, and how Hg ultimately enters wet deposition.

1.3 Study Goals

In 2006 an intensive monitoring campaign was undertaken in an industrial area in Eastern Ohio to collect data with the aim to improve our understanding of the physicochemistry of Hg in wet deposition. Specifically, the goals were to (i) quantify the soluble fraction of wet deposited Hg in an industrial area; (ii) investigate boundary layer removal of ambient gas and particulate pollutants during summer time precipitation events through case study analysis; and (iii) investigate the physical processes that determine the inclusion behavior of atmospheric Hg in to precipitation using aggregated sub-event sequential sampling.

2 METHODS

2.1 Sampling Site and Instrumentation Description

The monitoring site was established in October 2002, on the campus of the Franciscan University of Steubenville, Ohio (40°22’45.69”N, 80°37’10.29”W; 306 m above MSL). The site was selected with the specific aim of investigating the impact of coal combustion on the chemistry, transport and deposition processes of Hg. There are five large CFUBs within a 50 km radius of the site and seventeen within 100 km (Keeler et al., 2006). The site was equipped with continuous ambient gas, particulate matter, and meteorological instrumentation. A listing of the instruments applicable to the current discussion, as well as the sampling interval for each measurement is listed in Table 1. As part of the overall long-term study plan, a summer field

intensive was conducted July through September 2006, in part to investigate the physiochemistry of Hg wet deposition. During this period, an additional Tekran 2537a, 1130 and 1135 Hg speciation system was deployed and run asynchronously to provide continuous hourly data.

A more regionally representative site was added during this 2006 field intensive, 40 km to the west of STB (40° 29’ 30”N, 81° 09’ 26”W). This site, designated Steubenville West (STW), was situated in a rural area. With primarily western flow, STW provided a more regionally representative background site to compare STB Hg concentrations. Maps of the site locations and their proximity to CFUBs can be found in Keeler et al. (2006) and White et al. (2009).

2.2 Precipitation Collection and Analysis Methods

Comprehensive precipitation sample collection was conducted using several different methods to evaluate both soluble and insoluble fractions as well as scavenging and washout properties of Hg.

During the intensive, event samples continued to be collected as part of the long-term study (Keeler et al, 2006) with two sample trains (one for Hg and the other for trace element determination) housed in an automated wet-only precipitation collector (Landis and Keeler, 1997). A collocated automated wet-only precipitation collector configured with four sampling trains was deployed during the intensive for event-total filtration: two collocated Hg and trace elements trains were utilized to quantify sampling technique precision. The soluble fraction is operationally defined here as that which passes through a 0.2 µm pore size polycarbonate filter membrane (Morselli et al, 2003). The filtration was performed in real-time using vacuum chambers; sample bottles were placed inside the vacuum chambers immediately prior to rainfall, with the mouth of the bottle just below a 4 cm length of 6 mm O.D. FEP Teflon tubing fitted onto a filterpack housing. The sample collection funnels were connected to the filterpacks with acid-cleaned 1cm O.D. C-Flex™ tubing. Small electric Gast pumps pulled the vacuum from a port at the bottom of the chamber. All components of the sample trains were thoroughly acid cleaned prior to deployment; funnels and bottles were prepared as described in Landis and Keeler (1997).

Two wet-only MIC-B samplers equipped with Automated Sequential Precipitation Samplers (ASPS II) systems were deployed as part of the intensive. One was installed at the primary Steubenville site (STB) and the other was located at the upwind STW site. The ASPS II

is a modified version of the standard automated wet-only precipitation collector deployed as part of this study (Landis and Keeler, 1997). Added components include (i) 8-sample bottle (1L) racks with control valves to divert collected precipitation to specific bottles, (ii) an electronic controller and WLAN user interface to allow sampling parameter selection, and (iv) a data logger to collect ambient temperature, rainfall amount and other sample collection details. Figure 1 shows the main components of the system. The ASPS is routinely used to collect 8 daily event precipitation samples without operator intervention but can also be programmed collect true event precipitation, integrated precipitation, and split samples. The ability to split a single event by sample volume was utilized for this work.

The ASPS II collectors were programmed to sample sequentially throughout each individual precipitation event based on a minimum collection volume of 50 mL for each of the first 7 bottles, determined by depth accumulation recorded by the tipping bucket. The eighth and final bottle was set to collect until the end of the rain event. This configuration allowed sufficient volume for chemical analysis while maximizing the number of individual event sub samples. The ASPS II was configured with two sample trains, one each to be analyzed for Hg and trace elements. Two mL of 0.08M HCl preservative was added to each of the Hg sample bottles. The HCl preservative volume was scaled down from Landis and Keeler, 1997 based on the known sample volume of 50mL. Sub-event samples were collected for 12 weeks at STB and 5 weeks at STW during the summer of 2006; filtered samples were collected for 5 weeks, as the operation of this collection type demanded operator presence at time of precipitation (See Table 1). Twenty-three discrete events were collected at STB during the 12 week study, but only 14 will be examined here. Nine events were excluded because they had fewer than 4 splits or because the sample volume for one of the sub-event samples was less than 20 mL, the lower volume limit for blank contamination uncertainty.

Hg samples were oxidized to a 1% BrCl v/v solution, as determined gravimetrically, and stored in a dark cold room prior to analysis by cold-vapor atomic fluorescence spectrometer (CVAFS) using a Tekran Instruments (Knoxville, TN) Model 2600 (Landis et al., 2002). Trace element samples were acidified to a 0.2% HNO_3, 0.1 % HCl solution (v/v) and analyzed for 42 trace elements using a ThermoFinnigan (Bremen, Germany) Element2 high resolution magnetic sector field inductively coupled plasma mass spectrometer (HR-ICPMS) using the method detailed in Keeler et al.(2006).

2.3 Data Evaluation Methods

2.3.1 Individual Event Meteorology: Case Studies Analysis

A case-by-case precipitating event evaluation was performed on each set of sequential samples – aligning the sample collection times with wind and meteorological data along with ambient gas data enabled explanation of some variability in concentrations among samples. National Weather Service surface data plots were used for synoptic scale meteorological evaluation and system type determination. National Climatic Data Center (NCDC) archived Doppler radar (WSR-88D) data from Pittsburgh, Pa (KPBZ) was used to further identify path-history of precipitating cells impacting the STB site (Dvonch et al; 1998, White et al; 2009).

2.3.2 Statistical Analysis

IBM's SPSS v16 was used for univariate statistical summaries and linear regression analysis. B is used to denote slopes that were not standardized, while Beta is used to denote regressions that were standardized within SPSS. Nonparametric tests (Wilcoxon rank sum, Analysis of Variance, and Kruskal-Wallis) were run in SAS v9.3 and a level of significance of $\alpha = 0.05$ was used for all statistical procedures.

3 RESULTS AND DISCUSSION

3.1 Soluble Fraction

Collocated filtered samples (n=5) exhibited an absolute mean difference of 19% (1.4 ± 1.2 ng L^{-1}) for Hg concentration. For the paired (filtered and total, n=7) samples, 61% of the Hg concentration was in the soluble form, ranging from 43% for the sample collected on the afternoon of July 14, to 77% for the low Hg concentration event on July 12 (Figure 2). Based on a total event uncertainty of 9.8% (Landis and Keeler, 1997), the differences between the soluble and total Hg concentration are statistically significant for all but the July 12th event. The July 12th event also contained the lowest absolute concentration of all filtered events.

In Table 2, the solubility of quantified trace elements are presented and compared to that of Hg. The elements are listed in order of decreasing solubility, based on the percent soluble fraction of the total wet deposition. The beta coefficient between soluble and total concentrations is also given as an additional indication of degree of solubility. The coefficients are not standardized, as both populations, the soluble and total concentrations, are identical

analytes and any variability between the data sets needs to remain intact for adequate representation. Analytes shown here were chosen based upon known particle properties: fine nucleation mode particles associated with combustion processes are often formed via gas to particle conversion, tend to form oxides and are in the ultrafine mode (<1 μm in aerodynamic diameter) so they are highly soluble (Seinfeld and Pandis, 1998). Crustal elements, however, are typically coarse mode (>2.5μm) and are much less soluble (Seinfeld and Pandis, 1998).

As hypothesized, combustion products formed via gas to particle conversion had the highest degree of solubility. Both Se and S, largely products of coal combustion, were highly soluble, indicating that very little of these elements were in large particle form. The other extreme, La and Ce, which are crustal constituents, were not statistically analyzed in the same manner as the other metals because the soluble fraction in precipitation was below detection limit for all filtered samples. Method detection limits for La and Ce (3.7 and 4.1 ppt, respectively) were less than 10% of the event total wet deposited average concentrations for these elements (52.9 and 113.9 ppt, respectively, approximations in table calculated with maximum uncertainty). This indicates that a large percentage of these elements were in the coarse particulate mode. The contribution of the soluble fraction to total wet deposition is greater than 50% for several of the elements studied. This is in agreement with an urban and industrial wet deposition study in Italy, with a similar filtration and extraction method (Morselli et al, 2003). Hg falls at the lower end of the highly soluble group, indicating that while the majority of Hg in rain was incorporated either as gas phase inclusion or scavenging of small particles, large particle scavenging, perhaps windblown soil components and fugitive dust may also play a role. The relative solubility of Hg in the precipitation also indicates that the majority of wet deposited Hg is immediately available for uptake by biota.

3.2 Removal Processes and Sequential Sub-Event Samples

3.2.1 Summary Statistics

Event total Hg concentrations for the long term study (Oct 2002 – Mar 2008, n = 386) are plotted against event precipitation depth in Figure 3 (a-c). Here, a slope of -0.14 indicates Hg was available for uptake into the later stages of precipitation, as even large precipitation amounts were high in concentration, this is consistent with other locally influenced receptor site

sample evaluations (see Section 1.2(i)). A low coefficient of determination (0.13) indicates that only 13% of the variation in Hg concentration could be accounted for by dilution of large events. Mixed precipitation was somewhat less efficient at scavenging with slope of -0.08, while the relationship for snow was dominated by three large depth events, but neither relationship was significant.

The sequentially sampled events are depicted in Figure 4 (a-m), with the sub-sample Hg concentrations as a continuous line and the comparison of the volume-weighted mean (VWM) for the storm splits compared to collocated event total collection Hg concentration as columns on the left. Overall, the sub-event VWMs were not significantly different (based on non-parametric tests) than the collocated event total Hg concentrations. The Hg concentration trend differs by event, for example, events a-f and h all exhibited an increase in Hg at some point in the sequence, in events g and j-n the Hg concentration decreased through-out the event. Note that the y axes on the figures depict different scale magnitudes, since the events had markedly different concentrations.

3.2.2 Individual Event Meteorology: Case Studies Analysis

While every event was seemingly unique in Hg concentration, a trend emerged upon closer inspection: earlier (July) samples deposition rates (concentration reduction over the course of an event) were lower than those for samples at the end of the study (September). Slopes for the deposition rates ranged from a gain of 6.1 ng L^{-1} per sub-sample (Aug 28) to a loss of 4.2 ng L^{-1} per sub sample on September 28 (both significant). Therefore, in-depth investigations into groups of individual events from both July and September were conducted to elucidate the impact of meteorological and/or local ambient gas concentrations on deposition rates. For the individual events, wind speed and direction, ambient SO_2 and hourly speciated Hg concentrations were evaluated to determine linkages with Hg concentration behavior throughout the individual events. Synoptic weather patterns were explored to examine the larger meteorological context and its impact on concentrations. It should be noted, that while Steubenville is surrounded by several Hg emitting point sources, initial review of the speciated ambient Hg gas data does indicate that southerly surface winds bring the highest concentrations of both RGM and Hg(p).

July 4: Figure 4(a). Southerly winds were prevalent in the warm sector that produced the precipitation for this event, ahead of a cold front. The low and occlusion passed well north of the Great Lakes through central Ontario. There was a decrease in Hg concentration with the first three sequential samples, and an increase in sample concentration with sub-events four and five that did not coincide with rain rate, wind or ambient surface level SO_2 changes. Winds shifted from north through northwest to southwest where it remained through the majority of the event, a higher density of anthropogenic sources in that section was probably responsible for the increased concentrations.

July 12: Figure 4(b-d). The next three sets of sequential samples were all associated with a similar synoptic regime, a long NE to SW stationary front with preceding wind from the southwest, center of the low passing over central Michigan, but there was substantial abatement in precipitation events such that three discrete, separate events were collected. Surface winds were consistent S to SWS throughout all three events. For the duration of the first set of sub-event samples in the early morning (0:19 to 1:50 EST: 7/12 early AM), Hg concentrations in rain decreased in the initial stages, but increased for samples four and five before dropping again in the last portion of precipitation. Wind speed, direction, rate did not change to explain the higher concentrations for sub-samples four and five were not accompanied by changes in wind speed, direction or rain fall rate, but ambient SO_2 concentrations did increase slightly at the 5 minute interval corresponding to collection of these samples. Ambient concentrations dropped off significantly for all three Hg species throughout the course of this event.

Three hours later (4:50 EST: 7/12 AM), rain began again, this time associated with slightly increased wind speeds (same direction as for prior event) and Hg concentrations in precipitation were lower and remained relatively unchanged throughout the event (Figure 4c). It should be noted that the lowest event total Hg concentration collected at the Steubenville site for the entire study period was 3.3 ng L^{-1} (09/28/2005), and baseline (operationally defined at 5th percentile) is 6.1 ng L^{-1}, while samples collected at less industrially influenced receptor sites maintained lower baselines (approximately half) and exhibited minimum concentrations less than 1 ng L^{-1}. Two of the eight sub-samples collected during this event exhibited the lowest concentrations ever collected at Steubenville, indicating that wash-out of Hg in the earlier stages of precipitation may occur. All three species of ambient Hg concentrations were lower

preceding the precipitation than for the early AM event discussed in the prior paragraph, as was the event total wet deposition Hg concentration.

The July 12 afternoon event (13:04 to 14:29 EST: 7/12 PM) exhibited an increase in Hg concentrations in the middle of the event (Figure 4d), and was associated with decreased precipitation rate and a slight decrease in wind speeds. It was observed that the ambient particulate and RGM concentrations dropped below instrument detection limit by the end of the course of the three events. SO_2 was also significantly reduced. The three separate rain events on July 12 all occurred under the same synoptic pattern. Therefore, they could be considered sequential samples in and of themselves. The significant increase in total event Hg concentration for the afternoon event as compared to the morning (based on associated error) indicates that local scale source contributions likely impacted the Hg concentrations.

July 14: Figure 4(e). Precipitation sub-event Hg concentrations increased and peaked during the middle of this event, a short evening rain associated with a stationary front. The rain did not cause a decrease in ambient RGM, however the Hg(p) dropped to below instrument detection over the course of the precipitation. SWS winds increased slightly and corresponded to the peak in sample five.

Sept 1: Figure 4(i). As discussed in White et. al., 2009, this event had low overall concentrations and was associated with the rear NW quadrant of Hurricane Ernesto. Relatively strong NE winds brought about very low ambient Hg concentrations. Much lower rain rates than the July events were maintained throughout. A drastic reduction in SO_2 during the early stages of rain was mirrored by RGM and Hg^0, but not by Hg(p) which increased four-fold over the course of the rain. Over the eight hour period (20:38 to 5:01 EST), sub-event samples exhibited an increase in Hg concentration for the fourth sample, as well as a slight steady increase over the last 4 samples in the sequence, as possibly explained by the Hg(p) increase.

Sept 12: Figures 4(k) and 5. A light rain lasted for a full 15 hours (8:00 to 23:00 EST), and was associated with southerly winds flowing into a large low that was situated over Indiana for the majority of the precipitation event. A slight wind direction shift from approximately 185 to 195 degrees brought about an increase in SO_2 that coincided with a Hg peak in sub-event samples. Ambient Hg concentrations increased as well throughout the event, particularly RGM, which peaked at 69 pg m^{-3} for the hour ending at 17:00. These changes in both ambient and wet deposition Hg concentrations can be observed in Figure 5. It is apparent that a very slight

change in surface wind direction brought about a significant change in ambient Hg concentrations, and that the subsequent precipitation also increased in concentration at this time. After the precipitation, ambient Hg levels fell to background, but began to rise again at approximately 9:00 AM.

Sept 13 Figures 4(l) and 5. The event examined here followed the previous event and can also be seen in Figure 5. Light, steady winds were observed, and there was a distinct decreasing trend in Hg concentration in both ambient measurements and precipitation over the course of the rain. This series of two back-to-back events provides evidence of both increasing Hg concentrations over the course of a rain event associated with slight perturbations in local meteorology as well as decreasing Hg concentrations over the course of precipitation when the winds did not favor additional supply of boundary layer ambient Hg.

Sept 28 Figure 4(m). Another event discussed in White et al. (2009), a cold frontal passage brought about late morning rains (5:28 to 13:05 EST) on September 28. Winds shifting from south/southwest to north throughout the event were accompanied by the most drastic Hg concentration reduction rate in the 14 events depicted in Figure 4. A combination of wind shift and precipitation coincided with decreased SO_2 over the course of the event.

Overall, it was observed that local meteorological and ambient Hg may have played a role in the behavior of Hg concentration over the course of the events, and it was apparent that on several occasions, Hg concentrations increased at some point over the course of an individual event. It was seen on an individual event basis that minor perturbations in surface wind direction and speed may bring about conditions that favor an increase in ambient Hg concentrations due to impact of local sources and subsequent increases in sub-event sequential samples in the latter stages of precipitation.

3.2.3 Event aggregation

To better determine the overall wet deposition incorporation behavior of Hg, the events were examined together, in aggregate, and the Hg behavior was compared to that of other metals.

3.2.3.1 Rainfall Intensity

Often, an inverse relationship is evident between the concentration of an element in precipitation over time and the rainfall intensity (Lim et al, 1990), and it has been suggested that rainfall rate can be a dominating factor in determining wet-deposition flux (Lou, 2001). For this

study, rate was determined by the rain depth collected divided by the collection time, and a rate was applied to each sub-sample. Of the elements studied, only three exhibited statistically significant relationships between concentration and rainfall rate: Se, La and Ce; and Hg displayed no significant correlation (see Supplemental Data Table 1). This indicates that the physical or chemical properties and/or sources controlling Hg inclusion are not the same as the crustal elements. We reiterate that for the total event precipitation samples multivariate statistical analysis has indicated that both Se and Hg deposition to this receptor site are primarily from coal combustion sources (Keeler et al, 2006; White et al., 2012). Se is hypothesized to be emitted primarily in the gaseous form (Senior et al, 2010), is rapidly transformed via gas to particle conversion, and then deposited through precipitation in the particle form. Because Se and Hg did not display similar relationships in regards to rainfall rate and concentration, but are known co-emitted elements, it is evident that the microphysical/chemical process of incorporation of Hg into wet deposition differs from that of Se.

3.2.3.1 Scavenging Coefficients

The relative deposition rate of sub-event samples was evaluated to help elucidate the removal process: rapid reduction in concentration throughout an event indicates boundary layer wash–out removal of larger mode aerosols, in comparison, a constant concentration throughout an event would be indicative of gas-phase inclusion within cloud and/or continuous feed of the element into either the boundary layer below the cloud or continuous entrainment aloft (Lim, 1990). Somewhat analogous to the rates discussed in Sections 1.2 and 3.2.1, where the natural log of event total concentrations were regressed against depth of samples (Figure 3), individual event deposition rates can be calculated directly through the decrease in concentration over the course of an event: the scavenging coefficient. The scavenging coefficient, the slope of a simple linear regression of concentration versus the sub-event sequence, describes the rate of decrease in an analyte concentration over the course of a precipitating event. The rate at which an element is removed would be high (linear regression slope close to negative one and with logarithmic decrease) with a below cloud large particle rain-out, zero if the concentration remained unchanged throughout the event. Likewise, if the element investigated did not change in concentration throughout an event, it would be assumed that the samples contained a background, longer range transport signature. It may also by hypothesized that the lowest concentration collected during a sequential series may reflect a larger scale entrainment, as it

would reflect the cleanest, and potentially cloud-water like concentrations. When taken as a whole, the series of sequentially collected events exhibits a large range of concentrations (Figure 4), and had to be standardized to elicit an appropriate comparison.

Both element concentrations and sequence number were standardized using Eq. 1 for *i* event, *k* sequence *within* each event such that the (i) washout behavior was standardized without weight on absolute concentration, **and** (ii) the first and last sub-event sample were given equal and opposite weights, without regard or weighting to events with a disproportionate number of sub-events.

$$score_{i,k} = \frac{[analyte, sequence]_k - \mu_i}{\sigma_i} \quad (1)$$

Scavenging coefficients are graphically represented for S and Hg in Figure 6a and b and all analyte coefficients can be found in Table 3, and are listed in the order of rate. S, Ca, V, Se demonstrate the most efficient scavenging, but S has the highest coefficient indicating the most robust and consistent reduction trend in concentration throughout an event. As previously discussed (Section 3.1), the majority (>90%) of S in the precipitation is in the soluble form and therefore large particle washout is not the reason for the efficient scavenging behavior. The majority of S in wet deposition at Steubenville is attributed to coal combustion sources (Keeler et al, 2006; White et al., 2012). Hg was shown to be less soluble than S (61% and 95%, respectively). Therefore we are evaluating two species with the same source, but different physical and/or chemical properties and behaviors. The other coal tracer, Se, predicted to be 70% due to coal combustion, was 77% soluble and had a more similar scavenging rate to Hg (-0.425 for Se and -0.395 for Hg).

The vast majority of SO_2 is transported away from the emission source and is converted to the soluble form at < 4% an hour (Husar et al., 1978; Dittenhoefer and De Pena, 1978); such transport is abundantly evident in historic acid rain studies - high concentrations of sulfate in precipitation in remote areas, such as the Adirondacks, is explained by transport from Ohio River Valley industrial regions, conversion and subsequent deposition (Menz and Seip, 2004). Because SO_2 to SO_4^{2+} conversion and deposition processes have been extensively studied, comparison between S ($S=0.4413* SO_4^{2+} + 539$, $r^2 = 0.9855$, $p<0.0001$ in Steubenville precipitation) and Hg behavior over the course of a precipitating event in the vicinity of local

sources can shed some light on the incorporation of Hg into rain. The difference in scavenging efficiencies between Hg and S is illustrated in Figure 6a and b, where S is efficiently scavenged as indicated both by the slope (-0.733) and the degree of fit about the regression: note the virtual absence of data points in the lower left and upper right hand quadrants. The scavenging coefficient (slope) is lower for Hg (-0.395) and there are numerous data points in the lower left and upper right hand quadrants, indicating the commonality of an *increase* in Hg concentration throughout the course of a precipitating event. The difference in coefficient of determination for the scavenging rates of S and Hg is particularly significant; the measured values are much better estimated (r^2=0.537, $p<0.0001$) by the equation of fit for S, whereas Hg is not as well described (r^2= 0.156, $p<0.0001$) by the linear regression model, indicating that only 16% of the variance in Hg concentration over the course of the event can be explained by scavenging. Less than 4% of sulfur in coal-fired utility boiler plumes is in the soluble, particulate SO_4^{2-} form (Husar et al, 1978; Garland, 1978) in comparison to 67 ± 27% of Hg in the soluble RGM form (Stevens et al., 1996). Therefore, it is possible we observed a 'buildup' of ionic sulfate particles in the boundary layer between precipitation events acting as primary cloud condensation nuclei, which were washed out effectively and quickly in the initial stages of precipitation, and not replenished after wash out due to the low fraction of emissions in the soluble form. Hg, on the other hand, with the majority of emissions in the soluble form (RGM), and while some below cloud washout is evident and buildup between events is probable, is continuously available for uptake in an area of constant supply.

Hg concentrations for identical events were collected at the STB and STW sampling sites to further investigate the reason for the lower observed Hg scavenging coefficients. For the months of July and August, when samples were collected concurrently, the Hg scavenging rate observed here differs from the aggregate total of -0.395. A comparison of standardized results are presented in Figure 7, where it is clear that the STB sequential samples are much less precise about the trend line, high concentrations occur during the later stages of precipitation (upper-right quadrant) and low concentration samples may occur during the earlier stages (lower left quadrant). Hg concentrations for precipitation collected at STW, the "upwind" site, show significantly greater washout behavior, scavenging coefficient is -0.390 and -0.515 for STB and STW respectively, than for the STB. The systematic examination of sequential event behavior at different locations within a region of coal combustion source influence has concluded that a

soluble form of Hg is available for incorporation into precipitation on a local scale. Overall, physicochemical properties of Hg emissions result in unique deposition rates near point sources, providing evidence to the physicochemistry causing previously reported near source deposition enhancement of Hg.

4 CONCLUSIONS

(i) For the Steubenville summertime precipitation events collected during this study, Hg falls at the lower end (61%) of the highly soluble analytes, indicating that the majority of Hg in rain was incorporated either as gas phase inclusion or small particle scavenging. This also indicates that a significant portion of deposited Hg is immediately available for biota methylation at this site.

(ii) Case study analysis showed that at the Steubenville site, subtle changes in local meteorology, when surface winds favor transport from large local sources, increases in both ambient and wet deposited Hg in the latter stages of a precipitating event are evident, indicating that Hg wet deposition is not due to gas phase in-cloud diffusion alone.

(iii) Comparison of deposition rates across sub-event precipitation samples, both Hg to S (co-emitted pollutants) and Steubenville Hg to more regionally representative samples, indicates that in the vicinity of local sources, the soluble form of ambient Hg is continuously available for uptake throughout the entire course of a precipitating event. While we are not suggesting that below cloud processes dominate all uptake of Hg into wet deposition, we conclude that in the vicinity of local sources, our data provides evidence of increased uptake and subsequent enhancement over regional and/or global Hg concentrations.

This integrated analysis of sequentially sampled sub-event Hg wet deposition samples has provided the first glimpse into the physiochemical mechanisms responsible for observed near field deposition gradients reported in the scientific literature. Additional research will need to be undertaken to provide information for the proper parameterization of deterministic models under different meteorological (e.g., cold cloud precipitation processes) and source impact regimes.

5 ACKNOWLEDGEMENTS

This work has been funded wholly or in part by the U.S. Environmental Protection Agency Office of Research and Development through cooperative agreement R-82971601-0, and Student Services Contract EP07D000572. It has been subjected to internal Agency review and accepted for publication. The views expressed in this paper are those of the authors and do not necessarily reflect the views or policies of the U.S. Environmental Protection Agency. Mention of trade names or commercial products does not constitute an endorsement or recommendation for use. We thank Ali Kamal and Brie Van Dam (formally of UMAQL) for managing laboratory support operations and assisting with sample collection, and Dr. James Slater (Franciscan University) for on-site logistical support.

6 REFERENCES

Benoit, J.M.; Gilmour, C.C.; Mason, R.P.; The Influence of Sulfide on Solid-Phase Mercury Bioavailability for Methylation by Pure Cultures of *Desulfobulbus propionicus* (1pr3). *Environ. Sci. Technol.* **2001**, 35, 127 – 132.

Burke, J., M. Hoyer, G. Keeler, T. Scherbatskoy. Wet deposition of mercury and ambient mercury concentrations at a site in the Lake Champlain basin. *Water, Air Soil Pollut.*, **1995**, 80, 353-362.

Coscio, M. R.; Pratt, G. C.; Krupa, S. V. An automatic, refrigerated, sequential precipitation sampler *Atmospheric Environment.* **1982**, 16, 1939-1944.

Dittenhoefer, A.C.; De Pena, R.G.; A study of production and growth of sulfate particles in plumes from a coal-fired power plant. *Atmospheric Environment*. 1978, 12, 297 -306.

Dvonch, J.T.; Graney, J.R., Marsik, F., Keeler, G.J., Stevens, R.K. An investigation of source-receptor relationships for mercury in south Florida using even precipitation data. *Sci Tot. Environ*. **1998**, 213, 95-108.

Garland, J.A.; Dry and Wet removal of sulphur from the atmosphere. *Atmospheric Environment.* 1978, 12, 349-362.

Gatz, D.F.; Dingle A.N. Trace substances in rain water: concentration variations during convective rain, and their interpretation. *Tellus.* **1971**, 23, 14-27.

Graney, J.R.; Landis, M.S.; Norris, G.A. Concentrations and solubilities of metals from indoor and personal exposure $PM_{2.5}$ samples. *Atmos. Environ.* **2004**, 38, 237-247.

Gratz, L.E., Keeler, G, J., Sources of mercury in precipitation to Underhill, VT. *Atmos. Environ*. 45, **2011**, 5440-5449.

Gratz, L.E., Keeler, G. J., Al-wali, K. Long-term Atmospheric Mercury Wet Deposition at Underhill, VT. International Association of Great Lakes Research Conference. **2005**.

Hammerschmidt, C. R.; Fitzgerald, W. F. Methylmercury in freshwater fish linked to atmospheric mercury deposition *Environ. Sci. Technol.* **2006**, 40, 7764-7770

Houze, R. A.; Cloud Dynamics. Acedemic Press, **1993**.

Husar, R.B., Patterson, D.E., Husar, J.D., Gillani, N.V. *Sulfur Budget of a power plant plume.* Atmospheric Environment, **1978**, 12, 549-568.

Keeler, G.J.; Landis, M.S.; Norris, G.A., Christianson, E.M.; Dvonch, J.T. Sources of Mercury Wet Deposition in Eastern Ohio, USA *Environ. Sci. Technol*. **2006**, 40, 5874-5881.

Krupa, S. V. Sampling and physico-chemical analysis of precipitation: a review *Environmental Pollution.* **2002**, 120, 565-594.

Landis, M.S.; Keeler, G.J. Critical evaluation of a modified automatic wet-only precipitation collector for mercury and trace element determinations. *Environ. Sci. Technol.* **1997**, 31, 2610-2615.

Landis, M.S.; Vette, A.F.; Keeler G.J. Atmospheric mercury in the Lake Michigan basin: influence of the Chicago/Gary urban area. *Environ. Sci. Technol.* **2002**. 36, 4508-4517.

Lim, B.; Jickells, T.; Davies, T. Sequential sampling of particles, major ions and total trace metals in wet deposition. *Atmos. Environ.* **1990,** 25A, 745-762.

Lindberg S., Bullock, R., Ebinghaus, R., Engstrom, D., Feng., Fitzgerald, W., Pirrone, N., Prestbo, E., Seigneur, C., A Synthesis of Progress and Uncertainties in Attributing the Sources of Mercury in Deposition. *AMBIO* **2007**, 36, 19-31.

Lou, W. Wet-deposition fluxes of soluble chemical species and the elements in insoluble materials. *Atmos. Environ.* **2001**, 35, 2963-2967.

Menz, F.C.; Seip, H.M. Acid Rain in Europe and the United States: an update. *Environmental Science & Policy. 2004*, 7, 253-265.

Morselli, L.; Olivieri, P.; Brusori, B.; Passarini, F. Soluble and insoluble fractions of heavy metals in wet and dry atmospheric depositions in Bologna, Italy. *Environ. Pollution.* **2003**, 124, 457-469.

Sandroni, V., Migon, C., Atmospheric deposition of metallic pollutants over the Ligurain Sea: labile and residual inputs. *Chemosphere* **2002**, 47, 753 – 764.

Seinfeld, J. H., Pandis, S.N., Atmospheric Chemistry and Physics: From Air Pollution to Climate Change. Wiley Interscience. **1998.**

Senior, C., Van Otten, B., Wendt, J.O.L., Sarofim, A. Modeling the behavior of selenium in Pulverized- Coal Combusiton systems. Combustion and Flame, **2010**, 157, 2095-2105.

Sherman, L.S., Blum, J.D., Keeler,G.J., Kemers, J.D. Dvonch, J.T., Investigation of Local Mercury Deposition from Coal-Fired Power Plant Using Mercury Isotopes. *Environ. Sci. Technol.*, **2012**, 46, 382-390.

Stevens, R.K.; Zweidenger, R.; Edgerton, E.; Mayhew, W.; Kellog, R.; Keeler G.J.; Source Characterization in Support of Modeling the Transport of Mercury Emissions in South Florida. Presented at Measurement of Toxic and Related Air Pollutants Symposium, May 7-9, Research Triangle Park, NC, **1996**.

Van Metre, P.C. Increased atmospheric deposition of mercury in reference lakes near major urban areas. *Environ. Pollution*. **2012**, 162, 109 – 215.

White, E.M.; Keeler, G.J. Landis, M.S.; Spatial Variability of Mercury Wet Deposition in Eastern Ohio: Summertime Meteorological Case Study Analysis of Local Source Influences. *Environ. Sci. Technol.* **2009**, 43, 4946-4953

White, E.M.; Keeler, G.J., Landis, M.S.; Source type and region attribution for wet deposited Hg in Eastern Ohio, USA. *Environ. Sci. Technol.* (submitted).

Table 1: Applicable measurements: October 2002 – March 2008, Steubenville, OH.

Instrument	Measurement	Increment	STB Duration	STW Duration
Ambient Gases	SO_2 (ppb)	Continuous, 5 minute	Oct '02 – Mar'08	
Meteorological	Wind Speed (m/s) Wind Dir Temp, %RH	Continuous, 5 minute	Oct '02 – Mar'08	Jul '06 – Sept '06
Tekran 2537a	Hg^0 (ng/m^3)	Hourly, odd hours	Oct '02 – Mar'08	
1130	Hg^{2+} (pg/m^3)			
1135	Hg(p) (pg/m^3)			
		Hourly, every hour	Jul '06 – Sept '06	
MIC-B	Precipitation for Hg, Ion and Trace Elements	Daily Event	Oct '02 – Mar'08	Jul '06 – Sept '06
MIC-B ASPS II	Precipitation Sequential Sub-event Hg, Ion and Trace Elements	50 mL	Jul '06 – Sept '06	July '06 – Aug '06
MIC-B modified for Filtration	Precipitation for Soluble Hg, Ion and Trace Elements	Daily Event	July '06 – Aug '06	

Table 2: Soluble contribution to the total wet deposition and regression statistics of soluble to total species concentrations in summertime rain for Steubenville Ohio; elements are listed in decreasing order of soluble fraction (n=5).

	S	Na	Se	Ca	Mg	Hg	As	Mn	V	Cr	Fe	La	Ce
% Soluble	95	85	77	71	63	61	49	48	47	19	10	<7	<4
B	0.943	0.851	0.682	0.719	0.679	0.605	1.477	0.692	0.361	0.233	0.044	<0.20	<0.20
r^2	0.988	0.895	0.86	0.912	0.968	0.927	0.940	0.450	0.723	0.425	0.813		
p	0.001	0.015	0.023	0.011	0.003	<0.001	0.006	0.080	0.068	0.233	0.037		

Table 3: Sub-event element concentration scavenging rate coefficients, all values significant at a p<0.0001 level.

	S	Ca	V	Ce	Mn	La	Fe	Zn	Se	As	Hg	Na	Mg	Cr
B	-0.733	-0.597	-0.565	-0.547	-0.536	-0.504	-0.464	-0.467	-0.425	-0.412	-0.395	-0.394	-0.388	-0.343
r^2	0.537	0.357	0.320	0.300	0.287	0.245	0.215	0.218	0.182	0.169	0.156	0.155	0.150	0..118

Figure 1: Automatic Sequential Precipitation System (ASPS II), inside the MIC-B wet-only insulated cabinet. a. Electronic data interface controller b. Funnel down-tube, c. Splitter, d., Solenoid valves, e. Sample bottles, f. Sample rack.

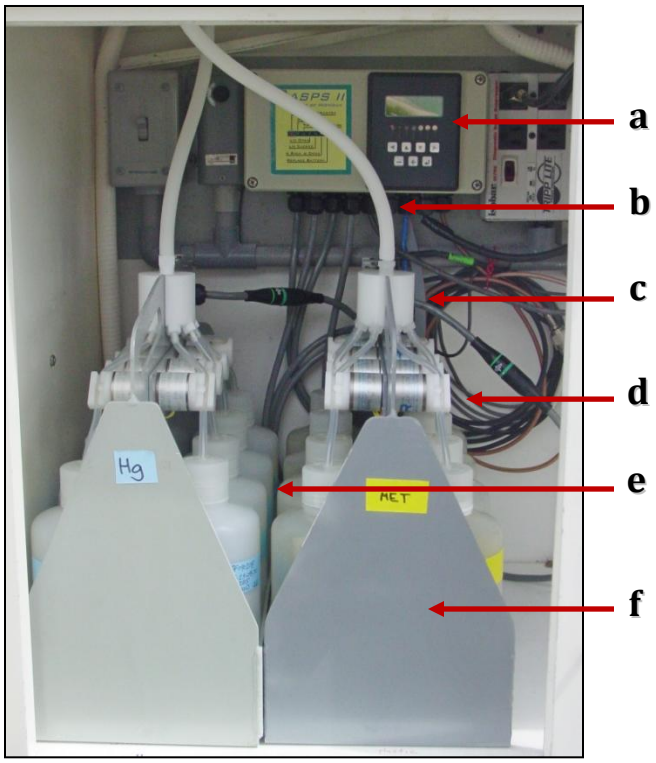

Figure 2: Soluble and total Hg wet deposition concentrations.

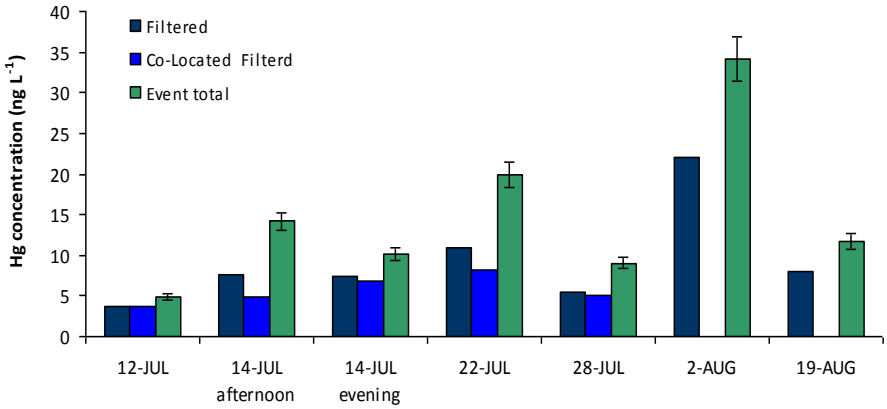

Figure 3 (a-c) Regression plots depicting precipitation depth and Hg concentration relationship, according to precipitation type.

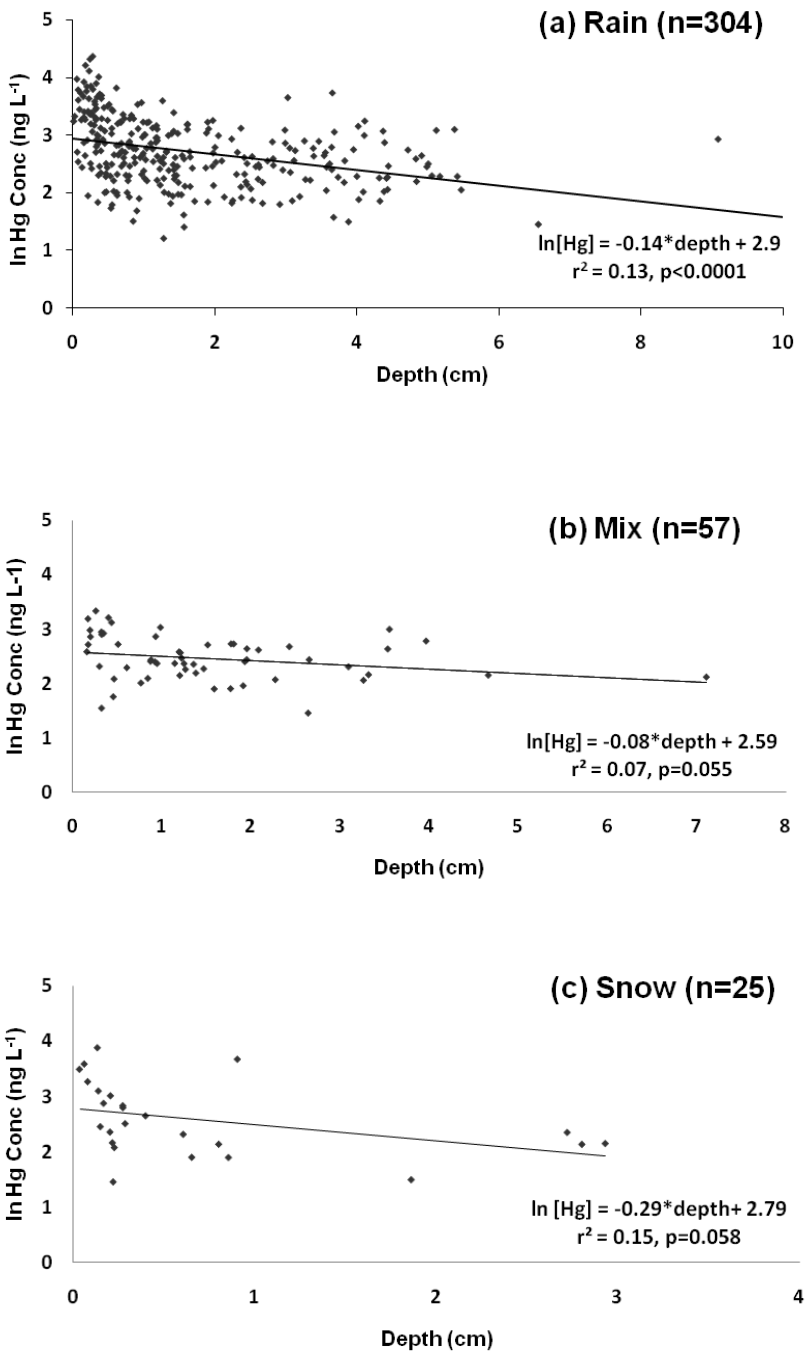

Figures 4 (a-m): Sub-event Hg concentrations in ng L^{-1}, total event concentration as columns, line represents Hg concentration through-out the course of a single event as discrete sub-samples, the blue line depicting the soluble fraction of the sub-event.

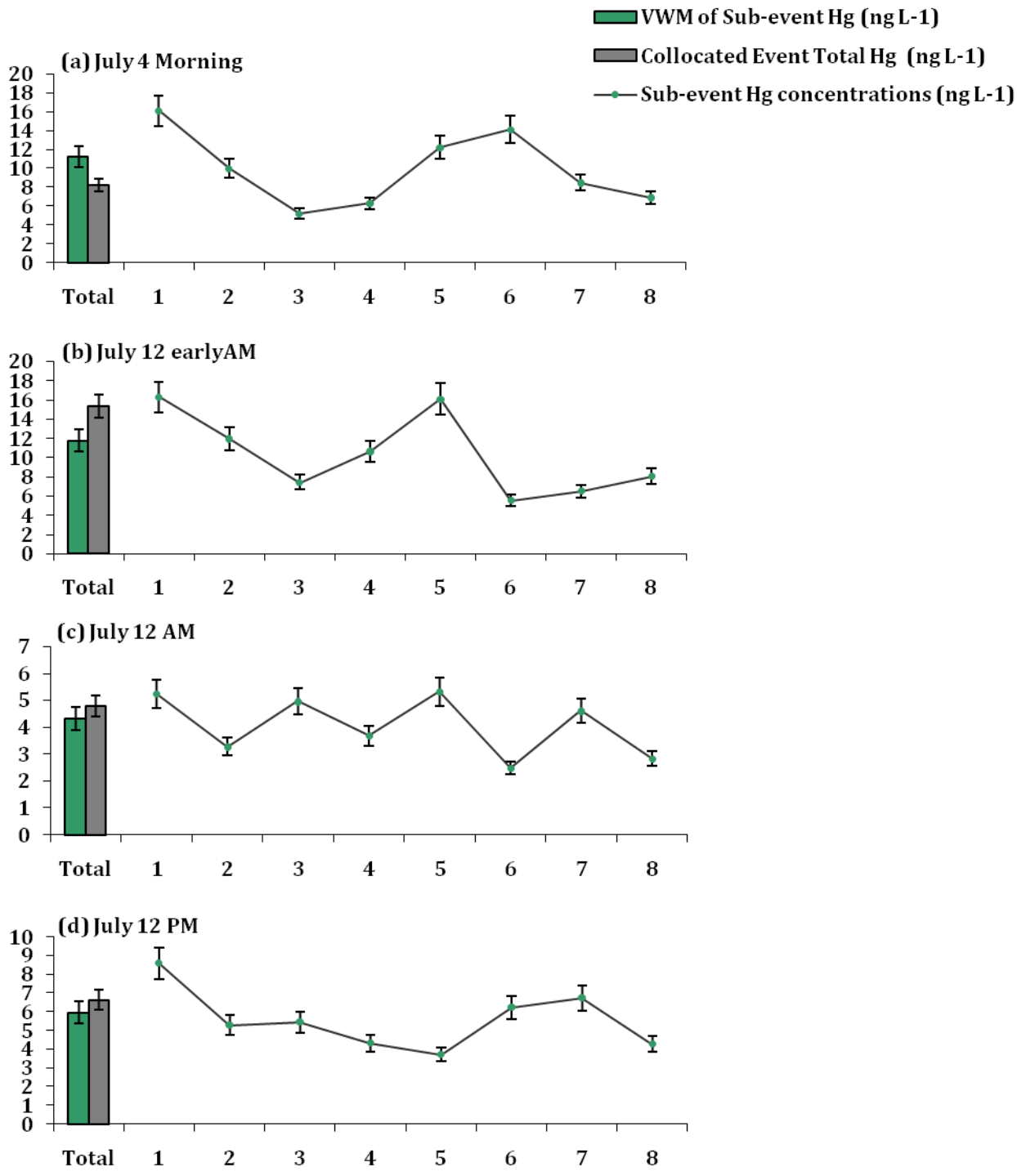

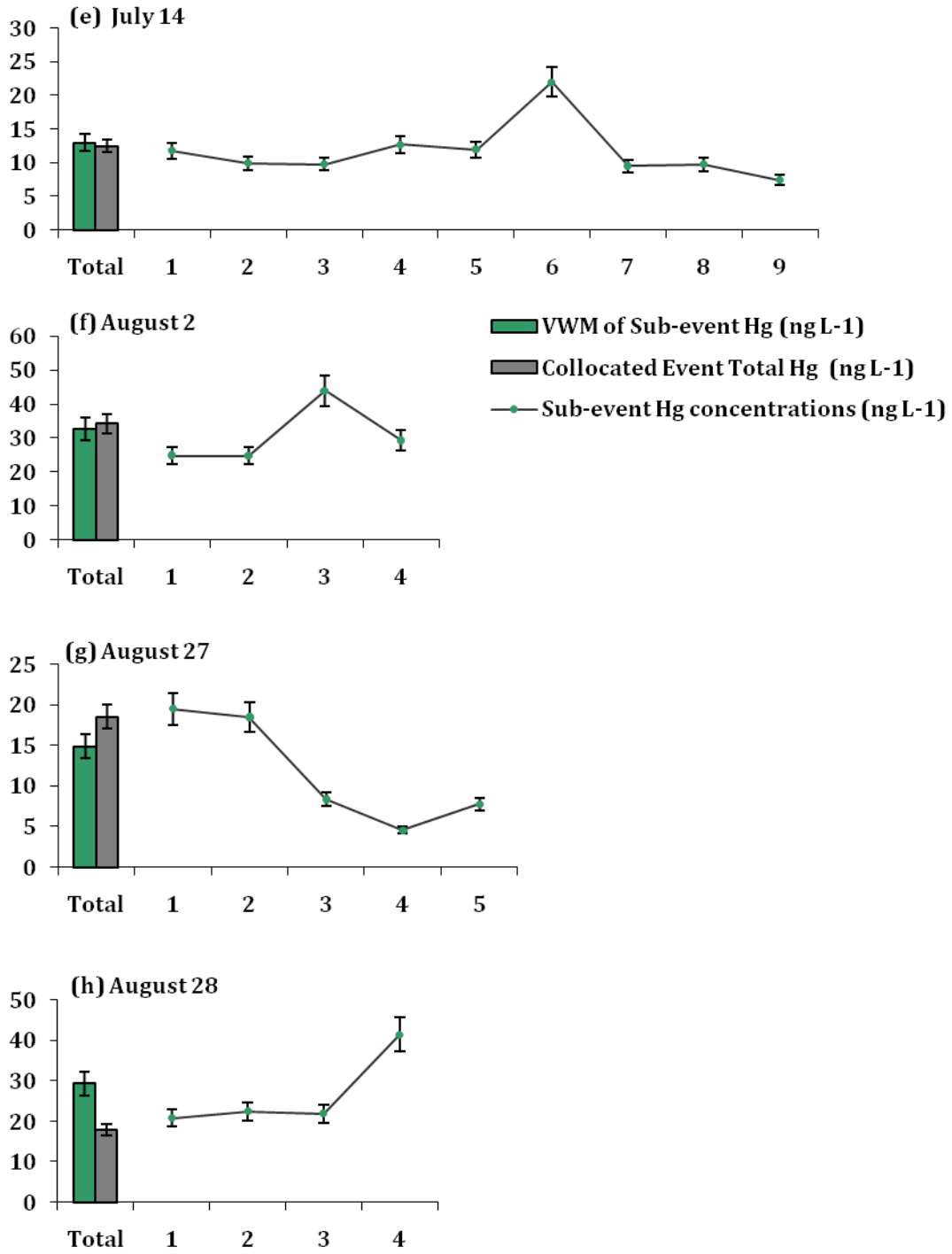
(e) July 14
30
25
20
15
10
5
0
Total
1
2
3
4
5
6
7
8
9
(f) August 2
60
50
40
30
20
10
0
Total
1
2
3
4
VWM of Sub-event Hg (ng L-1)
Collocated Event Total Hg (ng L-1)
Sub-event Hg concentrations (ng L-1)
(g) August 27
25
20
15
10
5
0
Total
1
2
3
4
5
(h) August 28
50
40
30
20
10
0
Total
1
2
3
4

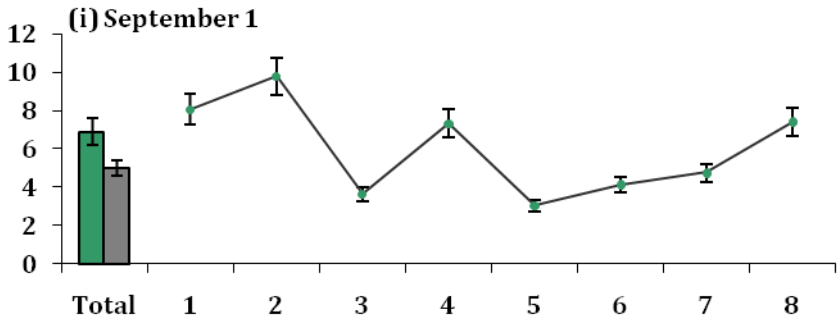
(i) September 1
12
10
8
6
4
2
0
Total
1
2
3
4
5
6
7
8

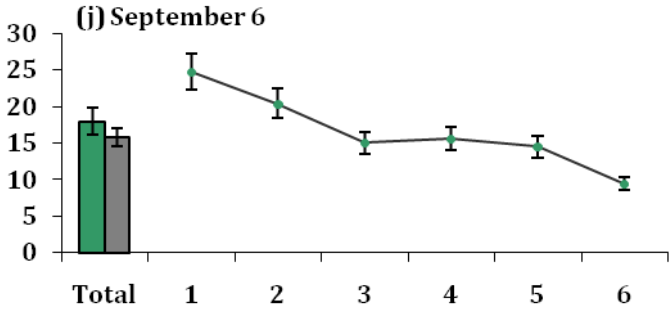
(j) September 6
30
25
20
15
10
5
0
Total
1
2
3
4
5
6

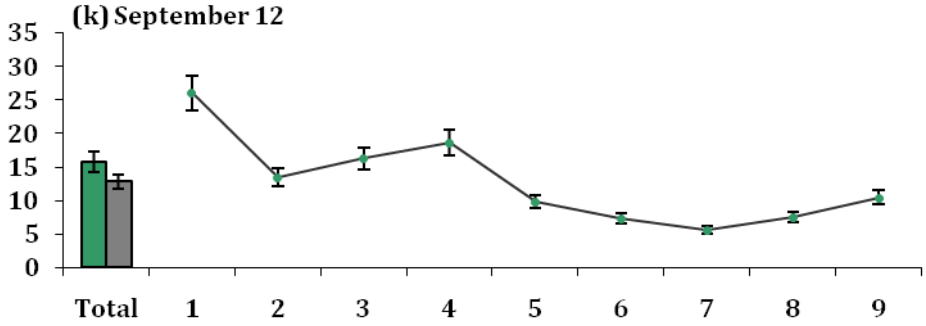
(k) September 12
35
30
25
20
15
10
5
0
Total
1
2
3
4
5
6
7
8
9

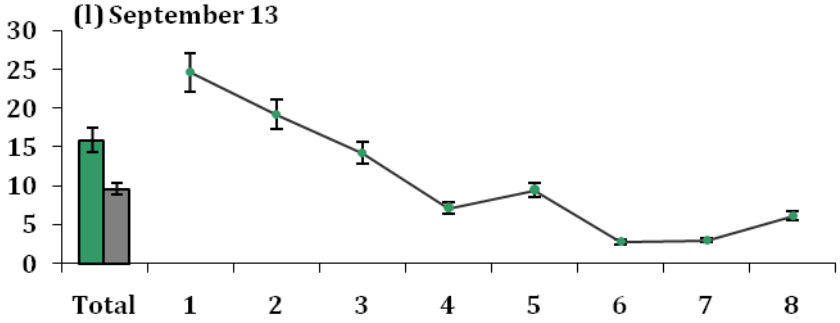
(l) September 13
30
25
20
15
10
5
0
Total
1
2
3
4
5
6
7
8

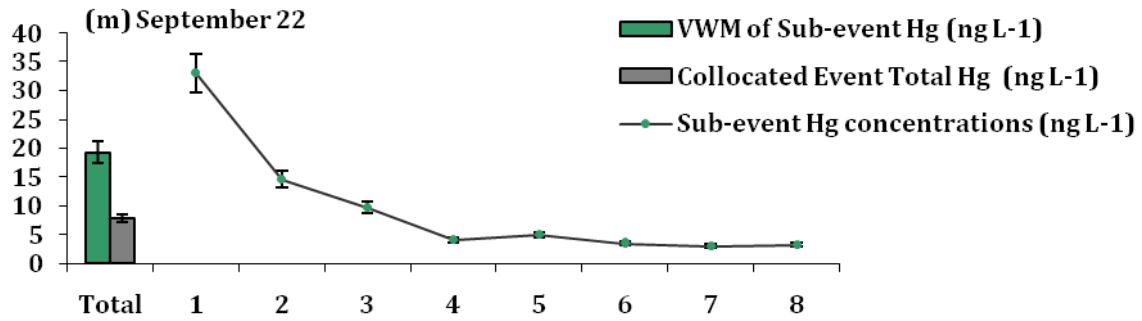
(m) September 22
VWM of Sub-event Hg (ng L-1)
Collocated Event Total Hg (ng L-1)
Sub-event Hg concentrations (ng L-1)
40
35
30
25
20
15
10
5
0
Total
1
2
3
4
5
6
7
8

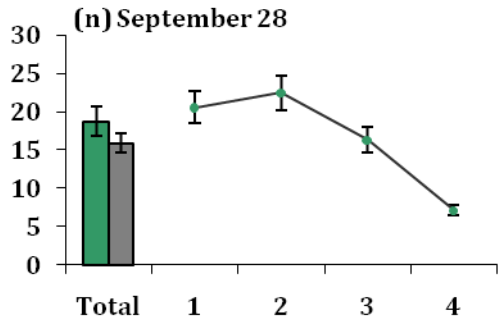
(n) September 28
30
25
20
15
10
5
0
Total
1
2
3
4

Figure 5: Ambient gas, winds and sub-event wet deposition Hg concentrations for a four day period in September 2006

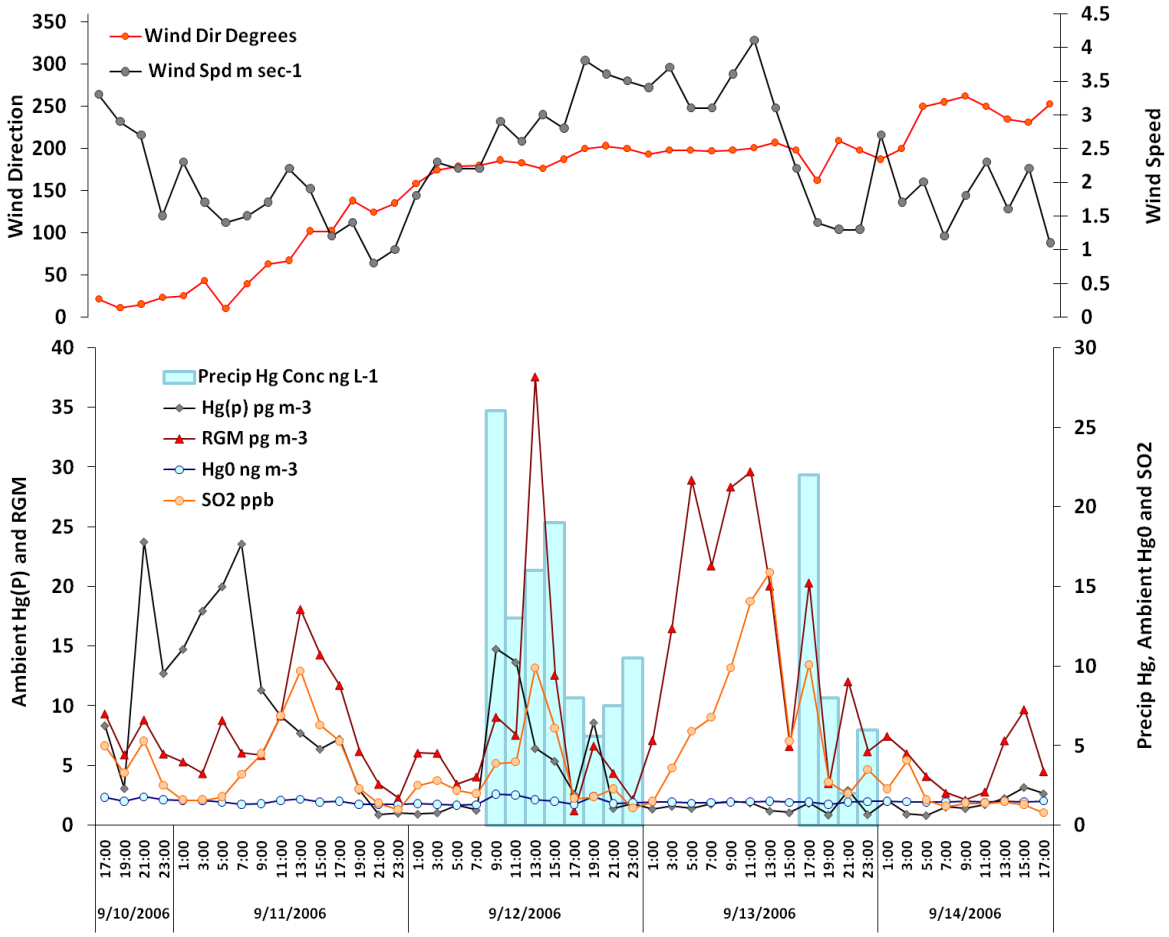

Figure 6: Three month sub-event standardized S and Hg concentrations.

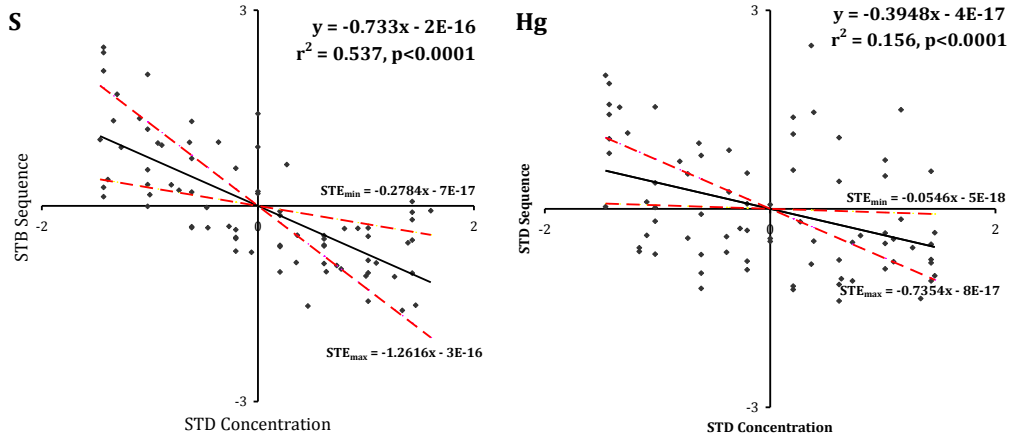

Figure 7: July sub-event standardized Hg concentrations at Steubenville (STB) and a rural site up-wind, west of Steubenville (STW).

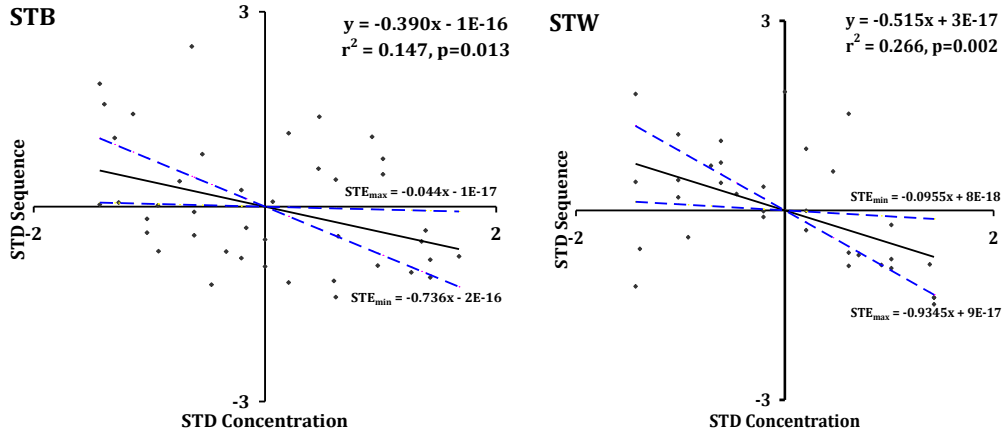

Supplementary Material

Click here to download Supplementary Material: Supplemental Data Splitsr.docx